Journal of Physics: Conference Series

PAPER • OPEN ACCESS

Development and Verification of an Improved Wake-Added Turbulence Model in FAST.Farm

To cite this article: E. Branlard *et al* 2024 *J. Phys.: Conf. Ser.* **2767** 092036

View the article online for updates and enhancements.

You may also like

- Vascularized adipose tissue engineering: moving towards soft tissue reconstruction
  Arne Peirsman, Huu Tuan Nguyen, Michiel Van Waeyenberge et al.
- DIFFUSE CLUSTER-LIKE RADIO EMISSION IN POOR ENVIRONMENTS
  Shea Brown and Lawrence Rudnick
- A CLUSTER PAIR: A3532 AND A3530
  Kiran Lakhchaura, K. P. Singh, D. J. Saikia et al.

This content was downloaded from IP address 192.174.37.51 on 12/07/2024 at 17:50

Journal of Physics: Conference Series **2767** (2024) 092036 doi:10.1088/1742-6596/2767/9/092036

Development and Verification of an Improved Wake-Added Turbulence Model in FAST.Farm

E. Branlard[1], J. Jonkman[2], A. Platt[2], R. Thedin[2], L. A. Martínez-Tossas[2], M. Kretschmer[3]

[1]University of Massachusetts Amherst, Amherst, MA, USA
[2]National Renewable Energy Laboratory, Golden, CO, USA
[3]Universität Stuttgart, Stuttgart, Germany

E-mail: ebranlard@umass.edu

Abstract. We introduce a generalized wake-added turbulence (WAT) model in the multiphysics, multiturbine simulation tool FAST.Farm. The WAT model introduces additional small-scale turbulence that represents the breakdown of vortical structures and shear layers in the wake. The article describes the development, implementation, calibration, and verification of the model. The novelties of the model include support for wake asymmetry, buildup of WAT across the wind farm, and secondary effects of wake-induced turbulence (e.g., wake meandering) driven by smaller-scale turbulence structures that arise from wake breakdown. Large-eddy simulations were run to support the calibration of the WAT parameters and verification of the model. Previous studies hypothesized that the lack of WAT modeling was the source of underprediction of fatigue loads, in particular for cases at low turbulence intensities and/or stable atmospheric boundary layers. This study confirms that the newly implemented WAT model enhances the loads predictions in these cases.

1. Introduction

Wake effects have a strong impact on the aeroelastic loads experienced by wind turbines in wind farms: wake deficits affect the mean wind speeds and wake-induced turbulence affects wind fluctuations. Aeroelastic simulations of multiple turbines in realistic atmospheric boundary layer (ABL) conditions are required to estimate loads impacted by wake and array effects. Such simulations are possible using conventional computational fluid dynamics such as large-eddy simulation (LES), but their computational expense has led the wind energy community to use simpler, computationally efficient engineering models that account for wake and array effects. For instance, the IEC 61400-1 design standard [1] describes the dynamic wake meandering (DWM) model, originally proposed in [2]. DWM implementations generally have three main submodels: wake-deficit evolution, wake meandering, and wake-added turbulence (WAT). The wake meandering model convects the wake deficit according to large turbulence scales of the ambient inflow. The WAT model introduces additional small-scale turbulence that represents the breakdown of vortical structures and shear layers in the wake. The main WAT effect is due to the individual and coherent tip and root vortices, but it is also caused by the secondary turbulent structures they form as they break down and interact with the main flow under phenomena known as vortex pairing, stripping, wandering, and various flow instabilities. The shear layers in the wake, combined with viscosity, also lead naturally to WAT.


Content from this work may be used under the terms of the Creative Commons Attribution 4.0 licence. Any further distribution of this work must maintain attribution to the author(s) and the title of the work, journal citation and DOI.
Published under licence by IOP Publishing Ltd

Previous versions of the DWM-based model FAST.Farm [3] did not include WAT. Comparison against results from LES and measured data indicated that the lack of WAT resulted in underprediction of fatigue loads, in particular for cases at low turbulence intensities and/or stable ABLs.

This work describes the development, implementation, calibration, and verification of a new WAT model in FAST.Farm aimed at improving load estimates in wind farms, particularly at low ambient turbulence intensity levels.

2. Wake-added turbulence model in FAST.Farm

2.1. Overview

The basic principle behind DWM and WAT models is illustrated in Figure 1. DWM models

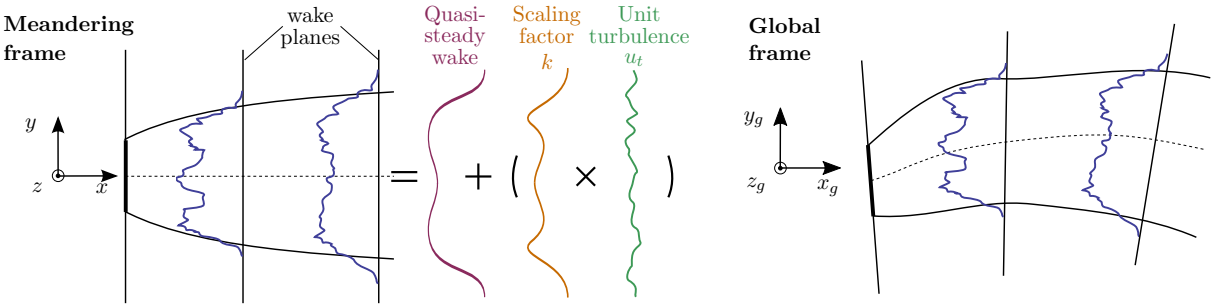

Figure 1. Wake deficit in the meandering frame (left) and global frame (right), according to the DWM model.

keep track of wake planes behind each wind turbine where the wake deficit is calculated and stored. The wake planes are convected and meandered according to the large scales of the background flow, and their orientation is based on the rotor orientation. By keeping track of the position and orientation of the wake planes, the DWM model can express the wake deficits in the global and meandering frames. The wake deficit ($\boldsymbol{u}_w$) in the meandering frame of reference (MFR) is assumed to consist of a quasi-steady wake component ($\boldsymbol{u}_{\text{qs}}$), computed using a thin-layer approximation of the Navier-Stokes equations, and a turbulent component ($\boldsymbol{u}_{\text{wat}}$). The latter is the WAT, and it is computed as the product of a scaling factor, k, multiplied by a unit-turbulence field $\boldsymbol{u}_t$. The unit-turbulence field consists of an isotropic turbulent field with unit standard deviations in each direction, obtained using the Mann turbulence model [4]. The scaling factor, k, is computed based on the quasi-steady velocity deficit and its radial gradient. Ultimately, the full velocity field at a given point consists of the superposition of the background flow ($\boldsymbol{U}$, usually known in the global frame) and the wake deficit ($\boldsymbol{u}_w$, usually known in the MFR):

$$\boldsymbol{u} = \boldsymbol{U} + \boldsymbol{u}_w, \qquad \text{with:} \quad \boldsymbol{u}_w = \boldsymbol{u}_{\text{qs}} + \boldsymbol{u}_{\text{wat}} \text{ and } \boldsymbol{u}_{\text{wat}} = k\boldsymbol{u}_t \tag{1}$$

In DWM models, the background flow is not influenced by the wind turbine wakes, which is referred to as a one-way interaction. General details on DWM models can be found in [2, 1]. The specific DWM implementation of FAST.Farm is described in [5]. The rest of this paper focuses on describing the WAT model.

The original WAT model is presented in [6]. We note that in WAT models, the turbulence is assumed to be unaffected by the local turbulence intensity and stability effects. In this work, we have introduced the following improvements:

- The scaling factor has been expanded to Cartesian coordinates to support non-axisymmetric wakes (e.g., curled wakes).
- The WAT is applied globally across the wind farm.

- WAT at the intersection of wakes in a wind farm is accounted for by superposing scaling factors across overlapping wakes.
- The isotropic turbulent field is convected at the mean wind farm wind speed and direction.
- The tuning constants of the model have been recalibrated against results from LES.
- The tuning constants are evolving as a function of the downstream distance.

The WAT model does not significantly affect the computational cost of FAST.Farm, and large wind farm simulations (30-100 turbines) are possible, though not demonstrated in this article. The following sections describe the different aspects of the implementation.

2.2. Calculation of the scaling factor in the MFR

In this section, we present the calculation of the WAT scaling factor in the MFR. In this frame, the coordinates are written (x, y, z) (see Figure 1), where x is, by definition, normal to a given wake plane. In the MFR, the DWM models typically assume that the background flow has slow time variations and moderate variation in the transverse direction. With these assumptions, the x-component of the velocity field at a given point is obtained from Equation 1 as

$$u_{\mathrm{DWM}}(x, y, z) = \overline{U} + u_{\mathrm{qs}}(x, y, z) + k(x, y, z)u_t(x, y, z) \tag{2}$$

where $\overline{U}$ is the spatially averaged and time-filtered ambient (without wakes) wind speed normal to the plane (see [5]), and where the time dependency has been omitted for simplicity. The subscript DWM will be omitted in the rest of this section.

The original WAT model [6] assumes that the additional turbulence introduced by the wake vortices is proportional to the wake deficit and the gradient of the wake. The original model assumes that the wake is axisymmetric, and the model is expressed in polar coordinates (x, r, θ) as follows[1]:

$$k(x, \tilde{r}) = k_{\mathrm{def}} \left| 1 - \frac{u(x, \tilde{r})}{\overline{U}} \right| + \frac{k_{\mathrm{grad}}}{\overline{U}} \left| \frac{\partial u(x, \tilde{r})}{\partial \tilde{r}} \right| = \frac{k_{\mathrm{def}}}{\overline{U}} \left| u_{\mathrm{qs}}(x, \tilde{r}) \right| + \frac{k_{\mathrm{grad}}}{\overline{U}} \left| \frac{\partial u_{\mathrm{qs}}(x, \tilde{r})}{\partial \tilde{r}} \right| \tag{3}$$

where k_{def} and k_{grad} are the two tuning constants of the model, respectively multiplying the quasi-steady wake deficit and the gradient of the wake deficit, and $\tilde{r}$ is the dimensionless radius, defined as $\tilde{r} = \frac{2r}{D}$, where D is the rotor diameter. In this work, we lift the assumption of axisymmetry. Therefore, the gradient of the wake deficit consists of two contributions from the gradients with respect to r and θ (also see [7]). After reintroducing the physical variable r (instead of $\tilde{r}$), our formulation takes the following form:

$$k(x, y, z) = \frac{k_{\mathrm{def}}(x)}{\overline{U}} \left| u_{\mathrm{qs}}(x, y, z) \right| + \frac{k_{\mathrm{grad}}(x) D}{2\overline{U}} \left[\left| \frac{\partial u_{\mathrm{qs}}(x, y, z)}{\partial r} \right| + \left| \frac{1}{r} \frac{\partial u_{\mathrm{qs}}(x, y, z)}{\partial \theta} \right| \right] \tag{4}$$

Based on our calibration study (see section 3), we have adapted the model so that the tuning parameters k_{def} and k_{grad} are functions of the downstream position instead of constants.

2.3. Unit-turbulence field

The WAT model relies on isotropic turbulence with unit standard deviations in each direction to introduce additional turbulence. In practice, this turbulence field is generated using the Mann model [4], and the turbulent field $\boldsymbol{u}_t$ is stored as a discrete four-dimensional (4D) array of shape $(3, n_x, n_y, n_z)$, where n_x, n_y, n_z are the dimensions in each of the global coordinates. The 4D array is referred to a turbulence box and will be further noted $\boldsymbol{u}_b(i_x, i_y, i_z)$. Turbulence boxes used in the wind energy community rely on Taylor's frozen hypothesis, which provides a relationship between space and time (also see subsection 2.4). Therefore, the x and time coordinates can be interchanged, and there is no need for an additional time dimension. The determination of the Mann model parameters is described below.

[1] The original model also uses the hub-height wind speed instead of the rotor average wind speed presented here.

The Mann model for isotropic turbulence depends on two main parameters: the turbulence length scale, L, and the scaled dissipation rate, $\alpha\epsilon^{2/3}$. Assuming the von Karman spectrum, Mann [4] obtained an approximation for the standard deviation of the turbulence as

$$\sigma^2 = \frac{9}{55}\frac{\sqrt{\pi}\,\Gamma(1/3)}{\Gamma(5/6)}\alpha\epsilon^{2/3}L^{2/3} \approx 0.688\alpha\epsilon^{2/3}L^{2/3} \tag{5}$$

where Γ is the Gamma function. Therefore, to generate a box with unit standard deviation, the dissipation rate needs to satisfy $\alpha\epsilon^{2/3} \approx L^{3/2}/0.688$.

As in the original WAT model, in this work we choose a length scale equal to the rotor diameter ($L = D$). For the grid spacing, it is expected that turbulence scales of the order of the chord length will affect turbine loads. Therefore, we approximate a representative chord length as $0.03D$ based on data from different wind turbines, and we choose this dimension for the grid spacing in all directions: $\Delta x = \Delta y = \Delta z = 0.03D$. The extent of the turbulence box is chosen as a compromise between covering a wide enough domain (to limit obvious periodicity in the signal) and limiting the disk and memory requirement. We set the extent in the longitudinal and horizontal directions as $L_x = L_y = 15D$, and in the vertical direction as $L_z = 2D$. The number of grid points is set to $n_x = n_y = 512$, $n_z = 64$ (based on the box extent and spacing and maintaining powers of 2 needed by the Mann simulator at Technical University of Denmark), leading to a box size of 65 Mb per wind component. Using the dimensions mentioned above (which are all proportional to the turbine diameter), we observed that the turbulence box generated by the Mann model is independent of the turbine diameter. Therefore, to simplify the user inputs, we provide a baseline turbulence box that can be used by default for any wind turbine. FAST.Farm then adjusts the spacing and extent of the baseline box based on the rotor diameter of the current simulation. If desired, users may provide their own turbulence box with different spacing and extent.[2]

2.4. Convection of the unit-turbulence box

Previous implementations of the WAT model [8] used one unit-turbulence box for each turbine. In our implementation, one box is used for the entire wind farm. This reduces the memory requirement and simplifies the implementation. We rely on the periodicity of the box in all space directions to compute the velocity at points outside of the domain of the turbulence box, which allows for a smaller box than the wind farm domain (see Figure 2). To relate space and time, the box is convected based on the mean rotor-averaged ambient velocity over all the turbines of the wind farm. This removes the need for additional user inputs and allows for convections that are not necessarily in the x-direction. In practice, FAST.Farm keeps track of a passive tracer (point $\boldsymbol{B}$), which can be thought of as the origin of the box, that convects according to

$$\frac{d\boldsymbol{B}}{dt} = \overline{\boldsymbol{U}}_{\text{farm}}(t), \qquad \overline{\boldsymbol{U}}_{\text{farm}} = \text{mean}\{\overline{\boldsymbol{U}}[i_w],\ i_w = 1 \cdots n_{WT}\} \tag{6}$$

where $\overline{U}[i_w]$ is the rotor-averaged ambient wind speed for turbine i_w, and n_{WT} is the number of wind turbines. The process is illustrated in Figure 2. For a fixed (Eulerian) point $\boldsymbol{P}$ in the wind farm, the indices mapping to the discrete unit-turbulence box are determined as if the point was at the location $\boldsymbol{B} + \boldsymbol{P}$. We have observed that linear interpolation within a turbulence box can filter out the turbulence. Therefore, we use nearest neighbor interpolation to obtain the value of $\boldsymbol{u}_t$. For instance, the index in the x-direction, at point $\boldsymbol{P}$ and at time t is determined as $i_x = \text{mod}\left[\text{nint}\left(\frac{P_x + B_x(t)}{\Delta x}\right), n_x\right]$. The unit-turbulence is then determined as $\boldsymbol{u}_t(t, \boldsymbol{P}) = \boldsymbol{u}_b(i_x, i_y, i_z)$, where $\boldsymbol{u}_b$ is the discrete turbulence field. We note that FAST.Farm uses

[2] For reference, we note that in Madsen et al. [6], the flow is assumed to propagate along the x-direction, and the following values are used: $\Delta x = 0.06D$, $\Delta y = \Delta z = 0.008D$, $L_x = 60D$, $L_y = L_z = 1D$, $n_x = 1024$, and $n_y = n_z = 128$.

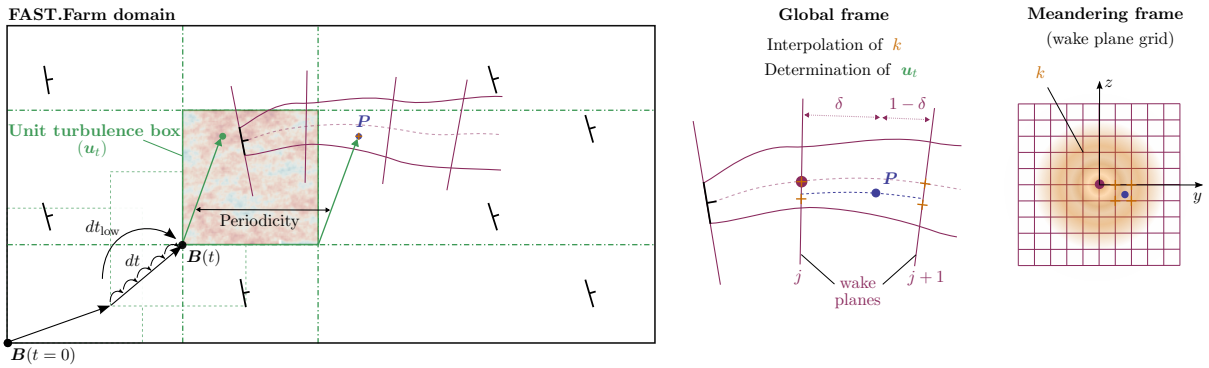

Figure 2. Illustration of the unit-turbulence box convection (left) and interpolation of k in between wake planes (middle) and within a wake plane (right).

two time steps, dt and dt_{low}, where the second is larger. To ensure that the WAT fluctuates at the highest frequency (relevant for loads), the box is convected at the smallest time step, dt.[3]

2.5. Interpolation of the k factor

Because the isotropic turbulence box is stored in global coordinates, the WAT contribution "$k\boldsymbol{u}_t$" is not computed in the MFR. This differs from other implementations. We compute the scaling factor k in the MFR and store it for each wake plane. When the full velocity field is constructed at point $\boldsymbol{P}$ (in global coordinates), the value of k is linearly interpolated based on the two wake planes (for instance of indices j and $j+1$) surrounding the point $\boldsymbol{P}$ (see the middle of Figure 2):

$$k(\boldsymbol{P}) = \delta(x)\, k_j(y,z) + [1-\delta(x)]\; k_{j+1}(y,z) \tag{7}$$

where (x,y,z) are expressed in the MFR. The interpolation factor δ is defined based on the position of the planes and the control point such that $\delta(x)=0$ if the point is on the plane j and $\delta(x)=1$ if the point is on the plane $j+1$. Because k is stored on a discrete Cartesian grid in each wake plane, 2D linear interpolation is used to obtain the value at an arbitrary point (y,z) in the wake plane (see the right of Figure 2). Linear interpolation is used for simplicity and to limit the computational time that would be required by higher order interpolations.

In FAST.Farm, calculations done in the MFR are carried out for each rotor's wake in parallel by the wake dynamics (WD) module, whereas the flow calculations performed in global coordinates, including wake merging, are done by the ambient and wind array effect module (AWAE). That is, k is computed in WD and interpolated in AWAE.

2.6. Wake overlaps

The case of multiple overlapping wakes is discussed in this section. We focus on the overlap of two wakes, with obvious generalization to multiple wakes. The case is illustrated in Figure 3. We consider a control point located between planes j and $j+1$ of wind turbine 1, and between planes k and $k+1$ of wind turbine 2. Equation 7 is applied individually to the wake of each turbine, using different interpolation factors δ_1 and δ_2 for each turbine, obtaining two values k_1 and k_2 at the point $\boldsymbol{P}$. A similar procedure is used in FAST.Farm to obtain the interpolated quasi-steady wake velocities at a given point. The merging of the quasi-steady velocity, as implemented in FAST.Farm, is documented in [9]. FAST.Farm performs a square-root average for the velocity normal to the wake planes and a regular sum for the transverse velocity components. Similar to the normal velocity component, we choose to use a square-root average: $k = \sqrt{k_1^2 + k_2^2}$.

[3] Internally, FAST.Farm updates $\overline{\boldsymbol{U}}_{\text{farm}}(t)$ at dt_{low}.

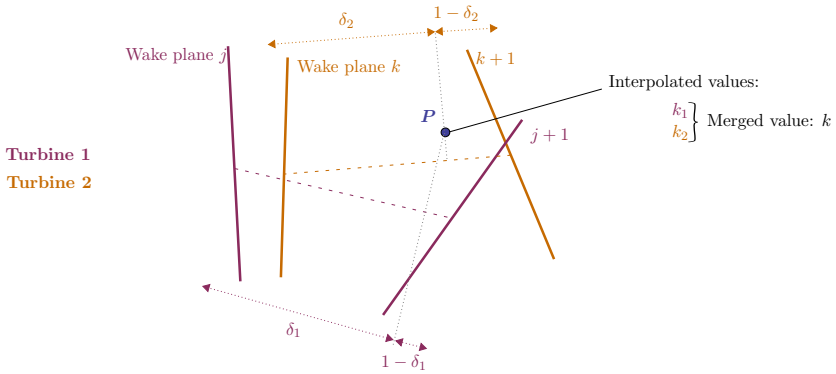

Figure 3. Intersection of wakes. Values of the scaling factor k (not shown) are interpolated at point P for each wake, before being square-root-averaged.

The procedure is generalized for the case of multiple wakes surrounding the control point as $k = \sqrt{\sum k_{i_w}^2}$ where the summation on i_w is done on the wakes that overlap at the control point.

3. Calibration using LES

To verify the validity of the model and its capacity to capture WAT effects, we carried out a calibration procedure based on results from LES, prior to implementing the model in FAST.Farm. We describe the calibration in this section.

3.1. Simulation setup

The baseline simulation setup involves the modeling of two International Energy Agency Wind Technology Collaboration Programme 15-MW reference wind turbines [10] spaced $7D$ apart. We perform LES using the actuator-line model in AMR-Wind of the ExaWind framework [11]. The onshore version of the turbine is used, and all relevant elastic degrees of freedom of OpenFAST are turned on. We use three cases, corresponding to three different canonical atmospheric stability conditions: stable, neutral, and unstable. The simulation conditions are summarized in Table 1. For the upstream turbine, and for all cases, the mean wind speed is $U = 8.0$ m/s, the mean rotor speed is 5.4 rpm, the pitch angle is zero, and the mean thrust coefficient is 0.7. The ROSCO controller [12] is used for both turbines. Using the baseline setup (two wind turbines),

Table 1. Mean conditions for the three LESs for the 3600-s period of interest. Turbulence intensity and turbulent kinetic energy are provided at hub height (150 m). Veer is expressed as a mean variation across the rotor area. Shear is given as the power law exponent.

Case	**Stable**	**Neutral**	**Unstable**
Turbulence intensity [%]	3.3	7.3	10.1
Turbulent kinetic energy [m^2/s^2]	0.10	0.51	0.98
Veer [deg/m]	0.023	0.019	0.002
Shear [-]	0.32	0.18	0.11

we also performed simulations with no wind turbines and with one wind turbine. For each simulation, velocity fields are extracted at a sampling frequency of 1 Hz at the global positions $x_g = [0, \cdots, 13]D$ in $1D$ increments behind the first turbine, resulting in a total of 14 output planes. The time series of structural loads for turbine components are extracted using regular OpenFAST outputs.

3.2. Postprocessing

Because the WAT model is developed in the MFR, we first postprocess the LES results to translate the output planes into this frame. We use the SAMWICH [13] toolbox to track the wake meandering at each downstream position and time step. The wake boundary and wake center are identified using two algorithms: a wake contour approach and an axisymmetric Gaussian fitting approach. We average the time series of wake center locations at each downstream plane and filter them using a moving average to reduce unphysical fluctuations occurring when the wake-tracking algorithm fails to identify the wake center. The output planes are then translated in the MFR using the wake center time series. An example of wake center time series and translated velocity field is given in Figure 4. Output planes of the no-turbine simulations are

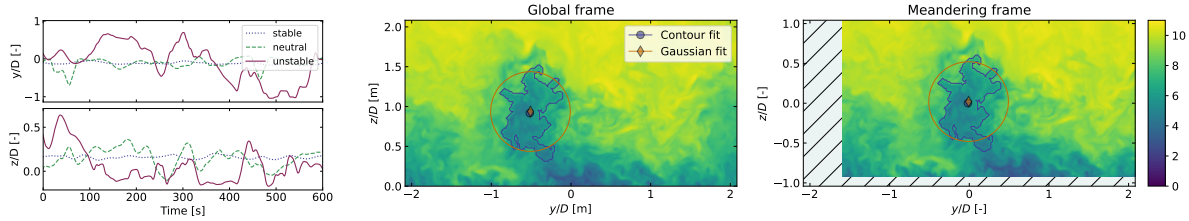

Figure 4. Wake trajectories obtained at $x = 6D$ for the different cases (left). Example of output plane velocity at $x = 6D$, showing the axial velocity for the neutral case in the global frame (middle) and the MFR (right).

also translated to the MFR, using the wake trajectories of the one- and two-turbine simulations.

3.3. Model fitting and calibration procedure

In this section, we consider horizontal velocity profiles in the MFR (i.e., at $z = 0$), and for ease of notation, we use the variable r instead of the variable y. From Equation 2, it is apparent that the variance of the velocity in the meandering frame of reference (assuming little time variation) reduces to the scaling factor k:

$$\mathrm{Var}\left[u_{\mathrm{DWM}}(x,r,t)\right] \approx k^2(x,r)\,\mathrm{Var}\left[u_t(x,r,t)\right] = k^2(x,r) \tag{8}$$

The DWM assumptions will not fully apply to LES in general because time dependencies of both the wake deficit and of the background flow will provide contributions to the variance of the flow. In the following, we neglect the first contribution, and assume that the flow field from the LES, in the MFR, can be decomposed as

$$u_{\mathrm{LES}}(x,r,t) = U(x,r,t) + \overline{u}_{\mathrm{qs}}(x,r) + u_{\mathrm{wat}}(x,r,t) \tag{9}$$

where U is obtained from the ambient simulation without wind turbines, $\overline{u}_{\mathrm{qs}}$ is computed as the mean velocity profile in the meandering frame over the entire time range of the simulation, and u_{wat} is defined as the remainder: $u_{\mathrm{wat}} = u_{\mathrm{LES}} - U - \overline{u}_{\mathrm{qs}}$. Under the decomposition of Equation 9, the variance (assuming negligible covariance) is

$$\mathrm{Var}\left[u_{\mathrm{LES}}(x,r,t)\right] = \mathrm{Var}\left[U(x,r,t)\right] + \mathrm{Var}\left[u_{\mathrm{wat}}(x,r,t)\right] \tag{10}$$

If the WAT model is valid, we expect Equation 8 and Equation 10 to be consistent, and therefore $\mathrm{Var}\left[u_{\mathrm{wat}}(x,r,t)\right] = k^2(x,r)$. Thus, to calibrate the model, we seek the tuning parameters k_{deg} and k_{grad} such that using Equation 4 (assuming an axisymmetric mean wake profile),

$$\sqrt{\mathrm{Var}\left[u_{\mathrm{wat}}(x,r,t)\right]} = \frac{k_{\mathrm{def}}(x)}{\overline{U}}\left|\overline{u}_{\mathrm{qs}}(x,r)\right| + \frac{k_{\mathrm{grad}}(x)D}{2\overline{U}}\left|\frac{\partial \overline{u}_{\mathrm{qs}}(x,r)}{\partial r}\right| = k(x,r) \tag{11}$$

The calibration procedure for each output plane ($x \in [0,\cdots,13]D$) in the MFR is therefore:'

(i) We compute the variance of the background flow, $\mathrm{Var}[U]$ using the simulation with no turbine.

(ii) For simulations with wind turbines, we compute the mean wake deficit, $\overline{u}_{\mathrm{qs}}(x, r)$ and apply a smoothing filter (mostly relevant for the unstable simulation) to limit the gradients. We then compute the gradient $\partial\overline{u}_{\mathrm{qs}}/\partial r$.

(iii) We calculate the variance of the "WAT" component using Equation 10, where negative values are set to 0.[4]

(iv) We perform a nonlinear fit of Equation 11 to obtain the tuning parameters.

In this work, we have performed parametric studies and experimented with different smoothing functions, and we have also tried the procedure either on the two-sided profiles $\overline{u}_{\mathrm{qs}}(y)$(with y positive and negative), or a one-sided profile, obtained by taking the mean of the profile on both sides of the x-axis. Overall, we have observed limited variations of the tuning parameters based on these options. The results we report in this article are taken as the average over the different studies we performed.

3.4. Calibrated parameters

Examples of fits obtained using the calibration procedure from subsection 3.3 are shown in Figure 5, using the one-turbine simulation case, double-sided horizontal velocity profile, and a Savitzky-Golay smoothing filter with a window length of $0.15D$.

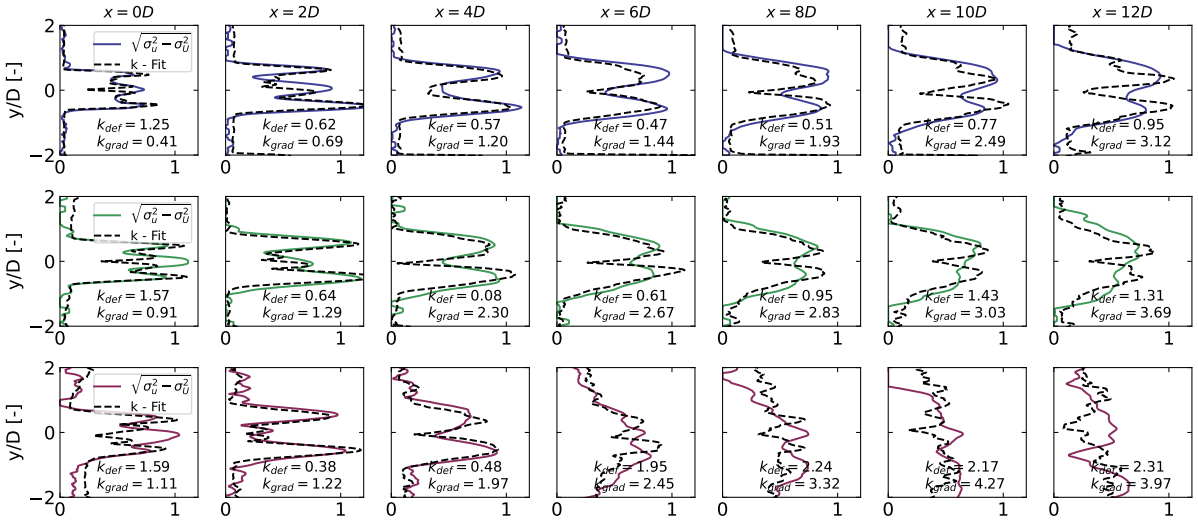

Figure 5. Example of fitting parameters obtained behind the wake of a single turbine for the different simulations: stable (top), neutral (middle), unstable (bottom). The x-axis represents $\sqrt{\mathrm{Var}\, u_{\mathrm{wat}}}$, with units in m/s. Similarity between the model ($\sqrt{\mathrm{Var}\, u_{\mathrm{wat}}} = k$) and the variance from LES ($\sqrt{\mathrm{Var}\, u_{\mathrm{wat}}} = \sqrt{\sigma_u^2 - \sigma_U^2}$) is an indication of validity of the WAT model given in Equation 4, that is, that the variance of the velocity in the meandering frame is proportional to the local wake velocity deficit and its gradient.

The quality of the fits is satisfying for the neutral and stable conditions over a wide range of downstream position. This indicates that the model provided in Equation 4 indeed captures the main features of the wake variance. Due to the strong decay of the unstable simulations, we estimate that the fitting parameters cannot be estimated beyond $8D$ for the unstable case.

We show the values of the fitted tuning parameters for the different stability cases in Figure 6.

[4] Alternatively, the variance can be computed from the time series of u_{wat}, but the approach is more computationally intensive.

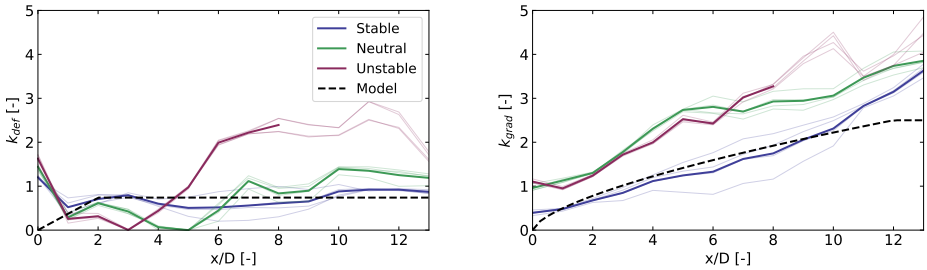

Figure 6. Fitted tuning parameters as a function of downstream distance for the different stability cases and for the one-turbine case. Values for different fitting options and smoothing are shown with lighter colors, and the averages are shown with darker colors. Results for the unstable case beyond $8D$ are uncertain due to the strong wake decay.

Based on the results from Figure 6, we develop an engineering model for the values of k_{def} and k_{grad}. We use the eddy viscosity filter model of FAST.Farm as a baseline function. This function is defined between f_{min} and 1 as

$$f(\tilde{x}, f_{\text{min}}, D_{\text{min}}, D_{\text{max}}, e) = f_{\text{min}} + (1 - f_{\text{min}}) \left[\frac{\tilde{x} - D_{\text{min}}}{D_{\text{max}} - D_{\text{min}}} \right]^e \tag{12}$$

where f_{min}, D_{min}, D_{max}, and e are parameters that affects the shape of f, and with $\tilde{x} = x/D$. The function is capped between f_{min} and 1 when $\tilde{x}$ is not between D_{min} and D_{max}. We propose the following models for the tuning parameters by choosing fits that work decently for the stable and neutral cases (considering that prior validations of FAST.Farm have shown that FAST.Farm already matches LES well for unstable cases and cases with high ambient turbulence, where a WAT model seems unnecessary[5]):

$$k_{\text{def}}(x) = 0.6\, f(\tilde{x}, 0, 0, 2, 1), \qquad k_{\text{grad}}(x) = 3.0\, f(\tilde{x}, 0, 0, 12, 0.65) \tag{13}$$

The two models are shown as dashed lines in Figure 6.

We chose to enforce a zero value at $\tilde{x} = 0$, as this is the expected behavior for a case with no background turbulence intensity. The progressive ramp-up of the k factors is characteristic of what would be expected as the vortices progressively break down downstream (see Figure 7).

4. FAST.Farm simulations results

In this section, we present results for the FAST.Farm implementation of the WAT model presented in section 2 with the calibration parameters derived in section 3.

4.1. Illustrative example without background turbulence

An illustration of the results from FAST.Farm with and without the new wake-added turbulence model is shown in Figure 7 for a simulation with a single wind turbine in uniform 8 m/s inflow. The WAT is seen to add granularity to the wake, resulting in a more visually appealing wake evolution, consistent with the expected behavior of a wake, with progressive buildup of turbulence downstream that mimics the vortex breakdown and breakdown of the shear layer, which will affect the loads of potential downstream wind turbines. We nevertheless note that FAST.Farm was not developed with the purpose of being run without background turbulence, especially considering that the WAT parameters were not calibrated for this situation. This test case is therefore only intended to show the effect of the WAT model, which is harder to visualize with background turbulence.

[5] We note that previous references used constant values for these coefficients, with different magnitudes from the ones obtained in our study. In [2], $k_{\text{def}} = 0.6$ and $k_{\text{grad}} = 0.35$. In [8], $k_{\text{def}} = 1.44$ and $k_{\text{grad}} = 0.84$.

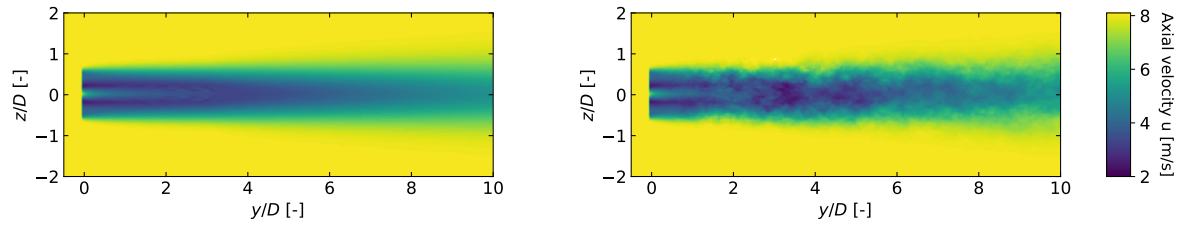

Figure 7. Instantaneous velocity field in the wake of one wind turbine in uniform 8 m/s inflow without (left) and with (right) WAT implemented in FAST.Farm.

4.2. Additional verifications

We performed (not shown here for brevity) the same procedure as the one presented in section 3, but using output planes results from FAST.Farm simulations instead of the LES results. As expected, the procedure returned values for k_{def} and k_{grad} that match the values used in the FAST.Farm model, thereby validating the implementation.

4.3. Comparison with LES

In this section, we perform comparisons between LES and FAST.Farm for the neutral and stable cases (most relevant for WAT), and the two-turbine simulation case. We extract the velocity field from the LES precursors (the simulation with no wind turbines) and store 30 min of velocity fields in the VTK format suitable to be used as FAST.Farm background flow input. We then run FAST.Farm simulations, with the same OpenFAST input files as the LES.

We compare the ratios of the damage equivalent loads between the downstream turbine and the upstream turbine. A ratio above 1 indicates that the metric is higher for the downstream turbine. Results are presented in Figure 8 for the different stability case and simulation setups: FAST-Farm without WAT ("FF No WAT"), FAST.Farm with WAT ("FF WAT") and LES. From

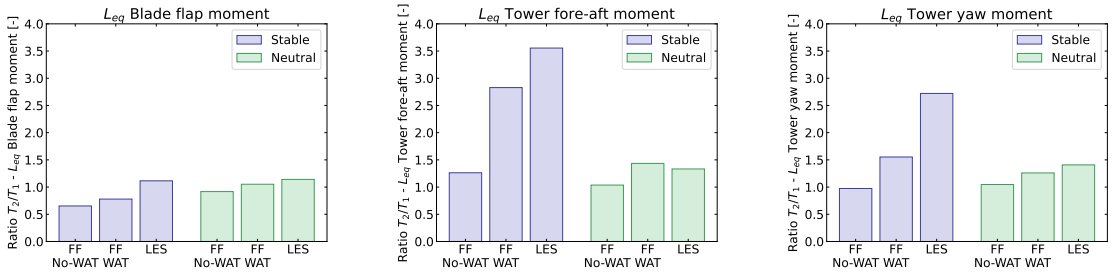

Figure 8. Ratios of damage equivalent loads between Turbine 2 (downstream) and Turbine 1 (upstream), for different stabilities and simulation tools (FAST.Farm with and without WAT, and LES). From left to right: blade flap moment, tower fore-aft moment, tower yaw moment.

the figure, we observe that the damage equivalent loads are increased when WAT is included in the FAST.Farm simulations. The effect is most significant in the stable case and for the tower loads. Despite an improvement, we observe that the damage equivalent loads from FF-WAT, for most of the results presented, are still lower than the ones predicted by LES. We note that in section 3, we calibrated the WAT parameters to match the wake parameters, whereas in this section we consider the difference in loads. Future work may therefore consider further calibrating the WAT parameters to match the loads on downstream turbines.

We expect the WAT to give additional asymmetry to wakes, provide a more realistic profile for wake breakdown, add additional turbulence scales impacting loads of downstream turbines (including secondary meandering associated with wake breakdown), and improve the comparisons of DWM to results from LES and measured data relative to prior DWM

implementations, particularly for stable ABL and/or low ambient turbulence conditions. Verifying these expectations will be the topic of future work.

5. Conclusions

In this work, we presented the development of a generalized wake-added turbulence (WAT) model in FAST.Farm, with novel contributions compared to existing models in the literature. The main effect of these new developments of WAT in FAST.Farm is the extension beyond polar coordinates and single wakes to enhanced WAT throughout the wind farm. This results not only in more visually appealing wake evolution but also in enhanced farmwide wake-added turbulence effects, including support for wake asymmetry, buildup of WAT across the wind farm, and secondary effects of wake-induced turbulence, e.g., wake meandering driven by smaller-scale turbulence structures that arise from wake breakdown.

A series of LES cases were run to support calibration of the WAT parameters and verification of the new WAT model implemented within FAST.Farm. Further calibrations are envisaged in the future, in particular to assess the impact of thrust coefficient, stability and turbulence intensity on the model, and to investigate the wake merging model.

These improvements will enable further wind farm design capabilities, with potential future applications in reducing wind farm underperformance and loads uncertainty, developing wind farm controls to enhance the operation of existing wind farms, optimizing the siting and topology of new wind farms, and innovating the design of wind turbines for the wind farm environment.

References

[1] International Electrotechnical Commission , *Wind energy generation systems - Part 1: Design requirements, IEC 61400-1, Edition 4,*. International Electrotechnical Commission, 2019.
[2] G. C. Larsen, H. A. Madsen, K. Thomsen, and T. J. Larsen, "Wake meandering: A pragmatic approach," *Wind Energy*, vol. 11, no. 4, pp. 377–395, 2008.
[3] K. Shaler and J. Jonkman, "Fast.farm development and validation of structural load prediction against large eddy simulations," *Wind Energy*, vol. 24, no. 5, pp. 428–449, 2021.
[4] J. Mann, "The spatial structure of neutral atmospheric surface-layer turbulence," *Journal of Fluid Mechanics*, vol. 273, pp. p141–168, 1994.
[5] J. Jonkman, J. Annoni, B. J. G. Hayman an, and A. Purkayastha, "Development of FAST.Farm: A New Multiphysics Engineering Tool for Wind Farm Design and Analysis," *AIAA SciTech 35th Wind Energy Symposium*, 2017.
[6] H. A. Madsen, G. C. Larsen, T. J. Larsen, N. Troldborg, and R. Mikkelsen, "Calibration and Validation of the Dynamic Wake Meandering Model for Implementation in an Aeroelastic Code," *Journal of Solar Energy Engineering*, vol. 132, 10 2010. 041014.
[7] E. Branlard, L. A. Martinez-Tossas, and J. Jonkman, "A time-varying formulation of the curled wake model within the fast.farm framework," *Wind Energy*, vol. 26, no. 1, pp. 44–63, 2022.
[8] M. Kretschmer, J. Jonkman, V. Pettas, and P. W. Cheng, "FAST.Farm load validation for single wake situations at Alpha Ventus," *Wind Energy Science*, vol. 6, no. 5, pp. 1247–1262, 2021.
[9] J. Jonkman and K. Shaler, "FAST.Farm User's Guide and Theory Manual," tech. rep., National Renewable Energy Lab., Golden, CO (US), 2020.
[10] E. Gaertner, J. Rinker, L. Sethuraman, F. Zahle, B. Anderson, G. Barter, N. Abbas, F. Meng, P. Bortolotti, W. Skrzypinski, G. Scott, R. Feil, H. Bredmose, K. Dykes, M. Shields, C. Allen, and A. Viselli, "Iea wind tcp task 37: Definition of the iea 15-megawatt offshore reference wind turbine," tech. rep., National Renewable Energy Laboratory, Golden, CO, USA, 3 2020.
[11] M. Sprague, S. Ananthan, G. Vijayakumar, and M. Robinson, "Exawind: A multifidelity modeling and simulation environment for wind energy," *Journal of Physics: Conference Series*, vol. 1452, p. 012071, 01 2020.
[12] NREL, "ROSCO. Version 2.4.1 - `https://github.com/NREL/ROSCO`," 2021.
[13] E. Quon, "Samwich-box - wake tracking,`https://github.com/ewquon/waketracking/`," 2023.

Acknowledgements
This work was authored in part by the National Renewable Energy Laboratory, operated by Alliance for Sustainable Energy, LLC, for the U.S. Department of Energy (DOE) under Contract No. DE-AC36-08GO28308. Funding provided by the U.S. Department of Energy Office of Energy Efficiency and Renewable Energy Wind Energy Technologies Office. The views expressed in the article do not necessarily represent the views of the DOE or the U.S. Government. The U.S. Government retains and the publisher, by accepting the article for publication, acknowledges that the U.S. Government retains a nonexclusive, paid-up, irrevocable, worldwide license to publish or reproduce the published form of this work, or allow others to do so, for U.S. Government purposes.